



Published in final edited form as:

*Urology*. 2013 June ; 81(6): 1265–1271. doi:10.1016/j.urology.2012.12.049.

## Multiphasic Enhancement Patterns of Small Renal Masses ( 4 cm) on Preoperative Computed Tomography: Utility for Distinguishing Subtypes of Renal Cell Carcinoma, Angiomyolipoma, and Oncocytoma

Phillip M. Pierorazio, Elias S. Hyams, Salina Tsai, Zhaoyong Feng, Bruce J. Trock, Jeffrey K. Mullins, Pamela T. Johnson, Elliot K. Fishman, and Mohamad E. Allaf

James Buchanan Brady Urological Institute, Johns Hopkins Medicine, Baltimore, MD; and the Department of Radiology, Johns Hopkins Medicine, Baltimore, MD

### Abstract

**OBJECTIVE**—To analyze the enhancement patterns of small renal masses (SRMs) during 4-phase computed tomography (CT) imaging to predict histology.

**METHODS**—One-hundred consecutive patients with SRMs and 4-phase preoperative CT imaging, who underwent extirpative surgery with a pathologic diagnosis of renal cell carcinoma (RCC), angiomyolipoma (AML), or oncocytoma, were identified from a single institution. An expert radiologist, blinded to histologic results, retrospectively recorded tumor size, RENAL (radius, exophytic/endophytic properties of the tumor, nearness of tumor deepest portion to the collecting system or sinus, anterior/posterior descriptor, and the location relative to polar lines) nephrometry score, tumor attenuation, and the renal cortex on all 4 acquisitions (precontrast, corticomedullary, nephrogenic, and delayed density).

**RESULTS**—Pathologic diagnoses included 48 clear-cell RCCs (ccRCCs), 22 papillary RCCs, 10 chromophobe RCCs, 13 oncocytomas, and 7 AMLs. There was no significant difference in median tumor size ( $P = .8$ ), nephrometry score ( $P = .98$ ), or anatomic location ( $P > .2$ ) among histologies. Significant differences were noted in peak enhancement ( $P < .001$ ) and phase-specific enhancement ( $P < .007$ ) by histology. Papillary RCCs demonstrated a distinct enhancement pattern, with a peak Hounsfield unit (HU) of 56, and greatest enhancement during the NG and delayed phases. The highest peak HU were demonstrated by ccRCC (117 HU) and oncocytoma (125 HU); ccRCC more often peaked in the corticomedullary phase, whereas oncocytoma peaked in the nephrogenic phase.

**CONCLUSION**—In a series of patients with SRMs undergoing 4-phase CT, tumor histologies demonstrated distinct enhancement patterns. Thus, preoperative 4-phase CT imaging may provide useful information regarding pathologic diagnosis in patients undergoing extirpative surgery.

The incidence of renal malignancy has increased dramatically during the past few decades, coincident with the increased use of axial imaging.<sup>1,2</sup> Small renal masses (SRMs), defined

Reprint requests: Phillip M. Pierorazio, M.D., 600 N. Wolfe St., Marburg 134, Baltimore, MD 21287. philpiorazio@jhmi.edu.

**Financial Disclosure:** The authors declare that they have no relevant financial interests.

as renal cortical tumors of less than 4 cm, now comprise upwards of 40% of all renal masses detected in the United States.<sup>3,4</sup> These SRMs frequently present a management dilemma: although most are renal cell carcinoma (RCC), 20% to 30% are benign, and those that are malignant are frequently low-grade with a low metastatic potential.<sup>2,5</sup> Despite the increase in diagnosis of SRMs—which are assumed to be early-stage disease—the number of deaths from RCC has not changed considerably during the past several years.<sup>2</sup>

Management options for patients with SRMs include active surveillance, partial or radical nephrectomy, and ablative technologies.<sup>6</sup> Treatment decisions are based on a risk/benefit ratio of surgical intervention vs baseline medical risks and life expectancy. Given the lack of a definitive diagnostic biomarker and the potentially limited diagnostic utility of percutaneous biopsy specimens, a combination of factors are typically used to approximate a tumor's aggressive potential. The typical hallmark of a SRM is the absence of macroscopic fat and the presence of enhancement in a solid renal lesion, without much attention given to the pattern of this enhancement. Axial imaging, including computed tomography (CT), has demonstrated some utility in distinguishing subtypes of RCC in large renal masses and may offer a noninvasive means of analysis of SRMs. To date, patterns of enhancement have not been rigorously tested for characterization of benign vs malignant disease and different subtypes of RCC within SRMs.<sup>7–12</sup> We therefore investigated the ability of multiphase CT enhancement to predict histology SRMs. This, along with other salient data, could potentially assist the urologist in making decisions regarding treatment.

## METHODS

The Institutional Urologic Surgery Database was queried for 100 consecutive patients undergoing extirpative surgery for a SRM (< 4 cm at pathology) who underwent multiphase, contrast-enhanced CT imaging at our institution between 2005 and 2011. Four-phase CT is the standard modality for evaluation of a renal mass at our institution. The technique is described in the Supplementary Materials. All patients had a pathologic diagnosis of RCC, oncocytoma or fat-poor angiomyolipoma (AML). One of 3 expert radiologists, blinded to the final histologic diagnosis, reviewed the 100 images, providing 3-dimensional tumor measurements, morphometric tumor description (according to the RENAL [radius, exophytic/endophytic properties of the tumor, nearness of tumor deepest portion to the collecting system or sinus, anterior/posterior descriptor, and location relative to polar lines] nephrometry score),<sup>13</sup> tumor, and cortical attenuation on all 4 acquisitions (precontrast, corticomedullary [CM], nephrogenic [NG], and delayed density).

Analysis of variance was used to compare patient and tumor characteristics in an attempt to distinguish RCC from benign disease and the 5 histologic diagnoses. Means were compared between groups using analysis of variance for more than 2 categories, and the *t* test or the Wilcoxon rank sum test was used for binary classifications. Polychotomous logistic regression analysis was used to compare the 5 histologic categories and calculate odds ratios and 95% confidence intervals, whereas binary logistic regression analysis was used to compare RCC vs noncancer.

## Image Selection, Interpretation, and Measurements

All scans were performed on a Sensation 16 or Sensation 64 multidetector CT scanner (Siemens Medical Solutions). Patients were routinely given 1000 mL water to drink during a 30-minute period before examination as a neutral oral contrast material. The intravenous contrast medium used was Omnipaque 350 or Visipaque 320 (both GE Healthcare Inc.). Contrast medium (100 to 120 mL) was injected at a rate of 3 to 4 mL/s, with arterial phases acquired at 25 to 30 seconds after the start of the injection and venous phases acquired at 60 to 70 seconds. Delayed scans were acquired at 5 to 10 minutes after injection. Scan parameters were 0.6- or 0.75-mm detectors with a slice thickness of 0.75 mm reconstructed at 0.5-mm intervals to achieve isotropic resolution. Routinely, 150 mA and 120 kVp were used. After scan data were processed, the scanner images were sent to a freestanding Leonardo work station (Siemens), where real-time postprocessing of the data set was performed.

Average tumor attenuation measurements were determined in each phase by dragging an ellipsoid cursor over the entirety of the SRM in the axial image demonstrating the largest diameter. Average cortical attenuation measurements were taken from the adjacent cortical tissue in the same image in which the SRM attenuation was determined. *Actual enhancement* was defined as the mean Hounsfield units (HU) in the given area of investigation. *Absolute enhancement* was defined as the difference in mean HU between the noncontrast phase and any given contrast phase (CM, NG, or delayed). *Percentage enhancement* was calculated as the mean HU in the tumor divided by the mean HU of the tumor in the noncontrast phase. *Relative enhancement* was defined as the difference between mean tumor enhancement and renal cortical enhancement during a given phase. *Cortical and medullary enhancement* was defined as the difference in average enhancement between the tumor and surrounding renal cortex or medulla, specifically. *Phase-specific enhancement* was defined as early, late, or pan-phasic if the greatest HU (>20 HU from baseline) was in the CM or NG, NG or delayed, or similar (−20 HU) among all phases, respectively.

## RESULTS

Pathologic diagnoses included 48 clear-cell RCCs (ccRCCs), 22 papillary RCCs (pRCCs), 10 chromophobe RCCs (chRCCs), 13 oncocytomas, and 7 AMLs. Patient and tumor characteristics are detailed in Table 1. There was no significant difference in median tumor size ( $P = .8$ ), nephrometry score ( $P = .98$ ), or anatomic location ( $P > .2$ ) among histologies (Supplementary Data). Sixty-eight patients were men. The ratio of men to women varied among tumor histology ( $P = .04$ ): men comprised 43%, 77%, 70%, 58%, and 91% of patients with, respectively AML, oncocytoma, chRCC, ccRCC, and pRCC.

Graphs and data depicting enhancement patterns are demonstrated in Figure 1 and the Supplementary Data. Significant differences were noted in actual enhancement ( $P = .007$ ), absolute enhancement ( $P < .001$ ), percentage enhancement ( $P < .001$ ), and phase-specific enhancement ( $P < .007$ ) by histology. Relative enhancement was not able to distinguish histology among phases.

Three distinctive patterns of enhancement were noted. pRCCs demonstrated a distinct enhancement pattern, with a low peak enhancement (average peak of 56 HU) and greatest enhancement during the NG and delayed phases. All pRCCs demonstrated an absolute enhancement of  $\geq 30$  HU in the CM phase, and 19 demonstrated an absolute enhancement  $\geq 40$  HU in the NG phase (Table 2). An actual enhancement cutoff of  $\geq 40$  HU yielded a sensitivity of 75% for predicting pRCC, and an absolute enhancement cutoff of  $\geq 20$  HU yielded a sensitivity of 70%.

The second pattern was of rapid, high attenuation with a thorough washout in the delayed phase and was indicative of ccRCC and oncocytoma. The highest peak HU were demonstrated by the ccRCCs (117 HU) and oncocytomas (125 HU); ccRCCs more often peaked in the CM phase, whereas oncocytomas peaked later in the NG phase. The third pattern, as demonstrated by AMLs and chRCCs, demonstrated an intermediate enhancement pattern compared with pRCCs and ccRCCs/oncocytomas.

Table 2 demonstrates the likelihood of a certain histology based on enhancement pattern during that phase. Of tumors demonstrating  $>80$  HU actual enhancement or  $>60$  HU absolute enhancement in any contrast-enhanced phase, 60%–70% were ccRCCs, 10%–20% were oncocytomas, and the remaining 10%–15% were AMLs, chRCCs, or pRCCs. ccRCCs comprised 92% of tumors with actual enhancement  $>140$  HU and 85.7% with absolute enhancement of  $>120$  HU. The preponderance of ccRCCs was less distinct in the NG phase, where only 70% of tumors with  $>120$  HU actual enhancement and  $>100$  HU absolute enhancement were ccRCCs. Oncocytomas demonstrated a preference for later enhancement compared with ccRCCs: 6 of 8 oncocytomas (75%) peaked in the NG phase (rather than the CM phase) compared with 14 of 34 ccRCCs (41%). In addition,  $>70\%$  of tumors that retained actual enhancement of  $> 80$  HU in the delayed phase were ccRCCs.

When logistic regression modeling was used to compare the 5 histologies, the strongest predictor of histology was the difference between the noncontrast and CM phase absolute enhancement (Table 3A). Although the analysis indicates that all histologies except chRCC exhibit significant differences compared with AML, the values are similar for ccRCC and oncocytoma, so the precontrast-to-CM change would not distinguish those 2 categories. Each 1-unit increase in the precontrast-to-CM change is associated with an 11% decreased likelihood of pRCC and a 4% increased likelihood of ccRCC or oncocytoma. When logistic regression was used to distinguish RCC from benign disease, the strongest predictor was the difference between tumor and medullary regions measured at the NG phase (Table 3B). A 1-HU difference between tumor and medulla during the NG phase is associated with a 2% increase in the risk of RCC compared with a benign histology.

## COMMENT

Although multiphasic CT imaging has proven useful for identifying benign vs malignant renal tumors and differentiating subtypes of RCC,<sup>9,11</sup> few studies have focused specifically on SRMs,<sup>8,14,15</sup> and no studies have rigorously evaluated 4-phase contrast-enhanced CT in these patients. We focused on patients with SRMs because they are most likely to benefit most from radiographic data that reflects histology.

Enhancement data in our study revealed 3 distinct patterns of attenuation. The concept of differing patterns of enhancement corresponding to histology is not novel and is based on tumor vascularity. Zhang et al<sup>12</sup> examined 198 patients with solid renal cortical tumors undergoing CT and concluded that ccRCC and oncocytoma were hypervascular, leading to rapid and early enhancement. That pRCC was mostly hypo-vascular, leading to low and delayed levels of enhancement, and that chRCC and AML enhanced moderately, correlating with intermediate levels of vascularity. Similarly, Jinzaki et al<sup>8</sup> correlated enhancement patterns with microvessel density within tumors <3.5 cm and concluded that ccRCC demonstrated peak enhancement of >100 HU and a high microvascular density, whereas chRCC and pRCC consistently demonstrated peak levels <100 HU and low microvascular density. Therefore, we build on this prior knowledge and report enhancement patterns in SRMs.

First, pRCC had the most distinct pattern, with relatively low levels of peak enhancement and relatively little fluctuation in attenuation from CM through the delayed phase. This pattern has been demonstrated in other studies of large pRCCs<sup>7,10</sup> as well as in a study of SRMs by Alshumrani et al.<sup>14</sup> Similar to Alshumrani et al,<sup>14</sup> where all pRCCs enhanced by 32 HU in the NG phase, most of the pRCCs in our series demonstrated low levels of absolute enhancement in the CM ( 30 HU) and NG ( 40 HU) phases. Although a number of studies have made strong assertions regarding pRCC using cut points for absolute enhancement<sup>10,14</sup> and enhancement relative to surrounding renal parenchyma,<sup>7</sup> we have found that although low levels of attenuation and little fluctuation across phases increase the likelihood of pRCC, this pattern does not exclude other tumor histology. However, tumors demonstrating a low, flat enhancement pattern have a >70% likelihood of being pRCC and >85% likelihood of being a malignant RCC as they weigh management options.

A second pattern of rapid, high attenuation enhancement that quickly washes out in the delayed phase was indicative of ccRCC or oncocytoma. Other studies have investigated and demonstrated patterns of enhancement for ccRCC and oncocytoma in larger renal masses<sup>9,12</sup>; however, these studies also relied on subjective measures. including the homo- or heterogeneity of the mass, presence of hypervascular peripheral components, central areas of low enhancement indicative of necrotic or cystic changes, the presence of calcification, and pattern of spread. Owing to the small and relatively homogenous appearance of the SRMs, we believe that these subjective measures are not particularly useful. In a study of SRMs, Jinzaki et al<sup>8</sup> demonstrated that ccRCC and oncocytoma showed a peak enhancement >100 HU, whereas other tumors enhanced to <100 HU. In a study attempting to distinguish oncocytoma from subtypes of RCC, Bird et al<sup>15</sup> found a percentage enhancement of 500% in the CM phase and a washout value of >50% to be predictive of oncocytoma. Although percentage enhancement could distinguish ccRCC and oncocytoma from other histologies in our series, it could not distinguish the 2 from each other (Table 2).

The proportion of histologic entities within our cohort closely resembles the relative incidence of benign and malignant histology for SRMs in existing reports.<sup>16</sup> Therefore, based solely on the incidence of a given histology, a SRM that demonstrates a high, early enhancement pattern has a higher likelihood of being ccRCC than oncocytoma, chRCC,

AML or pRCC. For all tumors in our study demonstrating >80 HU actual enhancement or >60 HU absolute enhancement in any contrast-enhanced phase, 60%–70% were ccRCC, 10%–20% were oncocytoma, and the remaining 10%–15% were other tumors. Increasing enhancement values during the CM phase increase the likelihood of ccRCC, as evidenced in the figure, incidence tables, and logistic regression. In addition, increasing HU in the NG decreased the likelihood of ccRCC and increased the risk of oncocytoma. Finally, even though we were not able to demonstrate the 50% washout as occurred in the study by Bird et al,<sup>15</sup> > 70% of tumors that retained actual enhancement of >80 HU were ccRCC. By carefully examining the enhancement pattern of SRMs, clinicians and patients can be more confident in selecting an intervention or conservative management of their mass.

Unfortunately, there was widespread crossover between benign and malignant histology within the third, intermediate pattern of enhancement. Similar to other authors, we were not able to distinguish benign from malignant lesions or subtypes of RCC in this range of enhancement.<sup>8,14</sup> Of SRMs with actual enhancement from 40–80 HU, 27%–41% were ccRCC and 3%–17.5% were benign. Most SRMs falling within the pattern of intermediate enhancement will be RCC, but this may not provide useful clinical data beyond what is known epidemiologically.

Previous studies have incorporated homogeneity, growth pattern, morphometric characteristics, and distinguishing features, such as calcification and cystic areas, to provide clues regarding tumor histology.<sup>7,9,11,14</sup> We did not find tumor morphology or other factors were useful in determining histology. This may be secondary to our relatively small sample size or reflect differences in the biology of small and large renal masses included in previous studies. A recent study by Kutikov et al<sup>17</sup> reported a nomogram to predict tumor grade and histology using the RENAL nephrometry score. Many tumors in this series were large and likely to be high-grade, ccRCC. In contrast to large masses, SRMs are more homogenous, represent a relatively smaller area within renal parenchyma, and lead to a more uniform sampling of pixels for HU measurements, which, in turn, may make it more difficult to discern differences in morphometry among histologies.

A number of additional factors might have influenced the classification of a SRM in our study. For instance, our study and previous studies have demonstrated different rates of tumor histology among men and women<sup>18</sup>; however, we were not able to correlate sex with enhancement. Potentially related to sex is the role of renal function and the estimated glomerular filtration rate, which may certainly affect absolute and dynamic enhancement patterns, explain some of the heterogeneity of enhancement patterns among individuals and tumors, and affect our ability to diagnose certain histologies. Similarly, we were not able to correlate high-grade tumors with differing enhancement patterns based on small sample size; nor were any tumors in this series papillary type 2 lesions. With larger sample sizes, it may be possible to detect more subtle differences among low- and high-grade variants of RCC.

This study has several limitations that deserve mention. The first is that variation in acquisition timing and technique can skew the interpretation of enhancement patterns and peak values. These variables can be referred to as extrinsic factors to indicate their relation to the CT protocol and not patient or tumor biology and can be minimized when using

standard CT protocols because they are equalized among a relatively large group of patients.<sup>10</sup> Second, although our radiologists were not provided the pathologic data, this study would be ideally performed in a prospective and truly blinded manner.

Finally, our study had a relatively small number of benign lesions, and there were a number of other benign SRM histologies that we did not include (ie, complex cysts, renal epithelial neoplasm of low-malignant potential, metanephric adenoma, etc.). These diagnoses are rare, and in the case of cysts, demonstrate distinctive CT findings leading to a diagnosis. We sought to investigate the most common SRM diagnoses in the hopes of characterizing malignancy in relation to benign disease and improving diagnosis and management in these patients.

Future studies should include larger populations, prospective multiobserver measurements, and further refinements of the actual predictive value of enhancement patterns in predicting histologic diagnoses. Inclusion of data from other facilities and different acquisition protocols will help to validate the applicability of the findings in this analysis. Nevertheless, dynamic enhancement data appear to give the urologist another hint at an underlying diagnosis. In an era with increased interest in active surveillance, future studies will determine whether adding multiphasic measurements to other available data (nephrometry score, sex, etc) would further refine our predictive ability with regards to SRMs.

## CONCLUSIONS

Multiphasic CT imaging may be useful in the prediction of histologic diagnosis in SRMs <4 cm, although a definitive diagnosis cannot be achieved by radiographic data alone. Distinctive enhancement patterns are apparent among different tumor histologies. Future studies are needed to determine whether adding multiphasic CT measurements to other available clinical data may improve the ability to obtain a diagnosis before selecting a treatment.

## Supplementary Material

Refer to Web version on PubMed Central for supplementary material.

## References

1. Hollingsworth JM, Miller DC, Daignault S, et al. Rising incidence of small renal masses: a need to reassess treatment effect. *J Natl Cancer Inst.* 2006; 98:1331–1334. [PubMed: 16985252]
2. Cancer Facts and Figures 2010. Atlanta, GA: The American Cancer Society; 2010. <http://www.cancer.org/acs/groups/content/@epidemiologysurveillance/documents/document/acspc-026238.pdf> [Accessed September 1, 2011]
3. Kane CJ, Mallin K, Ritchey J, et al. Renal cell cancer stage migration: analysis of the National Cancer Data Base. *Cancer.* 2008; 113:78–83. [PubMed: 18491376]
4. Nguyen MM, Gill IS, Ellison LM. The evolving presentation of renal carcinoma in the United States: trends from the Surveillance, Epidemiology, and End Results program. *J Urol.* 2006; 176:2397–2400. discussion 2400. [PubMed: 17085111]
5. Kutikov A, Fossett LK, Ramchandani P, et al. Incidence of benign pathologic findings at partial nephrectomy for solitary renal mass presumed to be renal cell carcinoma on preoperative imaging. *Urology.* 2006; 68:737–740. [PubMed: 17070344]

6. Campbell SC, Novick AC, Beldegrun A, et al. Guideline for management of the clinical T1 renal mass. *J Urol*. 2009; 182:1271–1279. [PubMed: 19683266]
7. Herts BR, Coll DM, Novick AC, et al. Enhancement characteristics of papillary renal neoplasms revealed on triphasic helical CT of the kidneys. *AJR Am J Roentgenol*. 2002; 178:367–372. [PubMed: 11804895]
8. Jinzaki M, Tanimoto A, Mukai M, et al. Double-phase helical CT of small renal parenchymal neoplasms: correlation with pathologic findings and tumor angiogenesis. *J Comput Assist Tomogr*. 2000; 24:835–842. [PubMed: 11105696]
9. Kim JK, Kim TK, Ahn HJ, et al. Differentiation of subtypes of renal cell carcinoma on helical CT scans. *AJR Am J Roentgenol*. 2002; 178:1499–1506. [PubMed: 12034628]
10. Ruppert-Kohlmayr AJ, Uggowitz M, Meissnitzer T, et al. Differentiation of renal clear cell carcinoma and renal papillary carcinoma using quantitative CT enhancement parameters. *AJR Am J Roentgenol*. 2004; 183:1387–1391. [PubMed: 15505308]
11. Sheir KZ, El-Azab M, Mosbah A, et al. Differentiation of renal cell carcinoma subtypes by multislice computerized tomography. *J Urol*. 2005; 174:451–455. discussion 455. [PubMed: 16006863]
12. Zhang J, Lefkowitz RA, Ishill NM, et al. Solid renal cortical tumors: differentiation with CT. *Radiology*. 2007; 244:494–504. [PubMed: 17641370]
13. Kutikov A, Uzzo RG. The R.E.N.A.L. nephrometry score: a comprehensive standardized system for quantitating renal tumor size, location and depth. *J Urol*. 2009; 182:844–853. [PubMed: 19616235]
14. Alshumrani G, O'Malley M, Ghai S, et al. Small (< or = 4 cm) cortical renal tumors: characterization with multidetector CT. *Abdom Imaging*. 2009; 35:488–493. [PubMed: 19536589]
15. Bird VG, Kanagarajah P, Morillo G, et al. Differentiation of oncocytoma and renal cell carcinoma in small renal masses (<4 cm): the role of 4-phase computerized tomography. *World J Urol*. 2011; 29:787–792. [PubMed: 20717829]
16. Storkel S, Eble JN, Adlaka K, et al. Classification of renal cell carcinoma: Workgroup No. 1. Union Internationale Contre le Cancer (UICC) and the American Joint Committee on Cancer (AJCC). *Cancer*. 1997; 80:987–989. [PubMed: 9307203]
17. Kutikov A, Smaldone MC, Egleston BL, et al. Anatomic features of enhancing renal masses predict malignant and high-grade pathology: a preoperative nomogram using the RENAL Nephrometry score. *Eur Urol*. 2011; 60:241–248. [PubMed: 21458155]
18. Pierorazio PM, Murphy AM, Benson MC, et al. Gender discrepancies in the diagnosis of renal cortical tumors. *World J Urol*. 2007; 25:81–85. [PubMed: 17066264]

## APPENDIX. Supplementary data

Supplementary data related to this article can be found at <http://dx.doi.org/10.1016/j.urology.2012.12.049>.



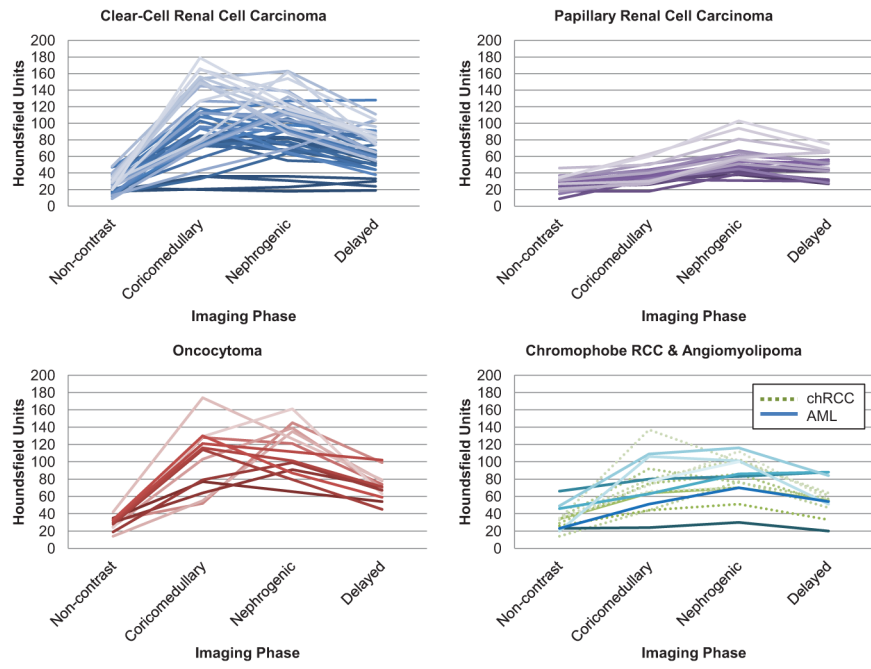


**Figure 1.** Patterns of enhancement on multiphasic imaging of 100 small renal masses by tumor histology. AML, angio-myolipoma; chRCC, chromophobe renal cell carcinoma. (Color version available online.)

**Table 1**

Patient and tumor characteristics of 100 consecutive patients undergoing extirpative surgery for a small, renal cortical tumor <4 cm

	Median (range) or No. (%)
Age, y	59.2 (16.1–78.9)
Men	68 (68)
Race	
African American	13 (13)
Caucasian	82 (82)
Other	5 (5)
CT tumor diameter, cm	2.6 (0.8–5.0)
Pathologic tumor size, cm	2.4 (0.7–4.0)
Histology	
Angiomyolipoma	7 (7)
Oncocytoma	13 (13)
Renal cell carcinoma	80 (80)
Clear-cell	48 (48)
Papillary	22 (22)
Chromophobe	10 (10)
Fuhrman Grade	
1	2 (2)
2	48 (48)
3	20 (20)

CT, computed tomography.

**Table 2**

Relative incidence of histology by Hounsfield units in each phase of imaging based on (A) actual enhancement and (B) absolute enhancement

HU	AML No. (%)	Oncocytoma No. (%)	chRCC No. (%)	ccRCC No. (%)	pRCC No. (%)
<b>(A) Incidence Table Based on Actual HU</b>					
Noncontrast					
>180–200					
>160–180					
>140–160					
>120–140					
>100–120					
>80–100					
>60–80	1 (100.0)				
>40–60	2 (22.2)	1 (11.1)		5 (55.6)	1 (11.1)
>20–40	3 (4.5)	10 (14.9)	8 (11.9)	29 (43.3)	17 (25.4)
0–20		2 (10.5)	1 (5.3)	12 (63.2)	4 (21.1)
Corticomedullary					
>180–200				3 (100.0)	
>160–180		1 (25.0)		3 (75.0)	
>140–160				6 (100.0)	
>120–140		4 (57.1)	1 (14.3)	2 (28.6)	
>100–120	2 (16.7)	3 (25.0)		7 (58.3)	
>80–100	1 (7.7)		3 (23.1)	9 (69.2)	
>60–80	2 (11.8)	3 (17.6)	3 (17.6)	7 (41.2)	2 (11.8)
>40–60	1 (8.3)	2 (16.7)	2 (16.7)	2 (16.7)	5 (41.7)
>20–40	1 (5.3)			4 (21.1)	14 (73.7)
0–20					1 (100.0)
Nephrogenic					
>180–200				1 (100.0)	
>160–180		1 (20.0)		4 (80.0)	
>140–160		1 (50.0)		1 (50.0)	
>120–140		3 (33.3)		6 (66.7)	

HU	AML No. (%)	Oncocytoma No. (%)	chrRCC No. (%)	ccRCC No. (%)	pRCC No. (%)
>100-120	3 (15.0)	1 (5.0)	3 (15.0)	12 (60.0)	1 (5.0)
>80-100	2 (11.1)	3 (16.7)	1 (5.6)	10 (55.6)	2 (11.1)
>60-80	1 (6.3)		4 (25.0)	7 (43.8)	4 (25.0)
>40-60			1 (7.1)	1 (7.1)	12 (85.7)
>20-40	1 (16.7)			3 (50.0)	2 (33.3)
0-20				1 (100.0)	
Delayed					
>180-200					
>160-180					
>140-160					
>120-140				2 (100.0)	
>100-120		1 (25.0)		3 (75.0)	
>80-100	3 (20.0)	1 (6.7)		11 (73.3)	
>60-80		8 (24.2)	2 (6.1)	18 (54.5)	5 (15.2)
>40-60	2 (6.7)	3 (10.0)	5 (16.7)	8 (26.7)	12 (40.0)
>20-40	1 (9.1)		1 (9.1)	4 (36.4)	5 (45.5)
0-20				1 (100.0)	
<b>(B) Incidence Table Based on Absolute HU</b>					
Corticomedullary					
>180-200				1 (100.0)	
>160-180				1 (100.0)	
>140-160				1 (100.0)	
>120-140		1 (25.0)		3 (75.0)	
>100-120		2 (22.2)	1 (11.1)	6 (66.7)	
>80-100	1 (10.0)	4 (40.0)		5 (50.0)	
>60-80		1 (12.5)		7 (87.5)	
>40-60	1 (6.3)	3 (18.8)	3 (18.8)	9 (56.3)	
>20-40	1 (7.1)	1 (7.1)	3 (21.4)	6 (42.9)	3 (21.4)
>0-20	3 (12.0)	1 (4.0)	1 (4.0)	2 (8.0)	18 (72.0)
-20 to 0				1 (50.0)	1 (50.0)
Nephrogenic					

HU	AML No. (%)	Oncocytoma No. (%)	chrRCC No. (%)	ccRCC No. (%)	pRCC No. (%)
>180-200				1 (100.0)	
>160-180				1 (100.0)	
>140-160				2 (50.0)	
>120-140		2 (50.0)		5 (71.4)	
>100-120		2 (28.6)		10 (83.3)	
>80-100	1 (8.3)	1 (8.3)		10 (52.6)	1 (5.3)
>60-80	1 (5.3)	3 (15.8)	4 (21.1)	6 (54.5)	1 (9.1)
>40-60	1 (9.1)	1 (9.1)	2 (18.2)	3 (14.3)	5 (23.8)
>20-40	1 (4.8)			3 (25.0)	7 (58.3)
>0-20	2 (16.7)			1 (100.0)	
-20 to 0					
Delayed					
>180-200				3 (100.0)	
>160-180				5 (62.5)	
>140-160				18 (75.0)	
>120-140				11 (30.6)	11 (30.6)
>100-120				8 (36.4)	11 (50.0)
>80-100				1 (4.2)	
>60-80		3 (37.5)		5 (20.8)	
>40-60	1 (4.2)	5 (20.8)	7 (19.4)	1 (4.5)	
>20-40	4 (11.1)	3 (8.3)	1 (4.5)		
>0-20		2 (9.1)			
-20 to 0	1 (50.0)				

AML, angiomylipoma; ccRCC, clear-cell renal carcinoma; chrRCC, chromophobe renal cell carcinoma; HU, Hounsfield units; pRCC, papillary renal cell carcinoma.

**Table 3**

Logistic regression models to distinguish **(A)** histology of small renal mass based on absolute enhancement between the noncontrast and corticomedullary phase and **(B)** renal cell carcinoma from benign histology using differences between tumor and medullary regions during the nephrogenic phase

<b>Histology</b>	<b>OR (95% CI)*</b>	<b>P Value</b>
<b>(A) Based on Corticomedullary Phase</b>		
AML	Reference	...
Papillary	0.89 (0.82–0.96)	.004
Clear-cell	1.04 (1.01–1.08)	.026
Chromophobe	1.02 (0.97–1.06)	.456
Oncocytoma	1.04 (1.00–1.08)	.043
<b>(B) Based on Nephrogenic Phase</b>		
Benign	Reference	...
RCC	1.016 (1.001–1.030)	.035

CI, confidence interval; OR, odds ratio.

\* Per 1 HU increase in difference.